ACS Infectious Diseases

pubs.acs.org/journal/aidcbc Article

Evaluation of EED Inhibitors as a Class of PRC2-Targeted Small Molecules for HIV Latency Reversal

Anne-Marie W. Turner, Raghuvar Dronamraju, Frances Potjewyd, Katherine S. James, Daniel K. Winecoff, Jennifer L. Kirchherr, Nancie M. Archin, Edward P. Browne, Brian D. Strahl, David M. Margolis,* and Lindsey I. James*

Cite This: *ACS Infect. Dis.* 2020, 6, 1719−1733 Read Online

ACCESS | Metrics & More | Article Recommendations | Supporting Information

ABSTRACT: A hallmark of human immunodeficiency type-1 (HIV) infection is the integration of the viral genome into host chromatin, resulting in a latent reservoir that persists despite antiviral therapy or immune response. Thus, key priorities toward eradication of HIV infection are to understand the mechanisms that allow HIV latency and to develop latency reversal agents (LRAs) that can facilitate the clearance of latently infected cells. The repressive H3K27me3 histone mark, catalyzed by the PRC2 complex, plays a pivotal role in transcriptional repression at the viral promoter in both cell line and primary CD4+ T cell models of latency. EZH2 inhibitors which block H3K27 methylation have been shown to act as LRAs, suggesting other PRC2 components could also be potential targets for latency reversal. EED, a core component of PRC2, ensures the propagation of H3K27me3 by allosterically activating EZH2 methyltransferase activity. Therefore, we sought to investigate if inhibition of EED would also reverse latency. Inhibitors of EED, EED226 and A-395, demonstrated latency reversal activity as single agents, and this activity was further enhanced when used in combination with other known LRAs. Loss of H3K27me3 following EED inhibition significantly increased the levels of H3K27 acetylation globally and at the HIV LTR. These results further confirm that PRC2 mediated repression plays a significant role in the maintenance of HIV latency and suggest that EED may serve as a promising new target for LRA development.

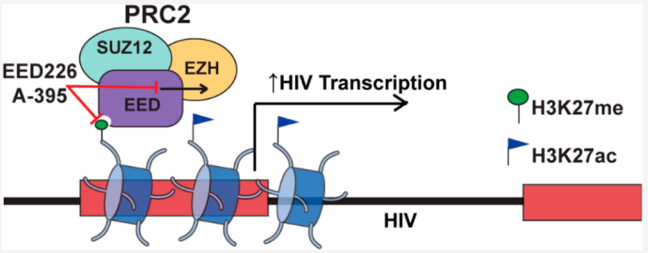

KEYWORDS: *HIV, latency reversal agents, EED, PRC2, polycomb, chromatin*

The integration of HIV into the host genome results in persistent, transcriptionally silent infected cells that remain despite treatment. While reactivation of the latent HIV population followed by clearance (so-called "kick and kill") remains a leading strategy for eradicating HIV infection, our understanding of the cellular pathways and epigenetic states that lead to latency is incomplete. Recent clinical testing of single latency reversal agents (LRAs), such as inhibitors of histone deacetylases, have shown promise in their ability to increase HIV transcription and reactivate the provirus from latency.[1] However, as single agents, LRAs have not yet altered proviral expression across the diverse population of persistently infected cells to the extent that is likely to be required for recognition and clearance of the latent reservoir. Thus, it seems likely that multiple pathways that either activate HIV transcription or remove restrictions to HIV expression must be targeted to achieve a clinically significant effect on the persistent viral reservoir. To do so, a greater understanding of the epigenetic mechanisms contributing to latency must be achieved in parallel with the discovery of novel small molecule inhibitors as potential LRAs.

Polycomb group proteins are involved in gene silencing, development, stem cell self-renewal, and differentiation.[2,3] Polycomb repressive complex 2 (PRC2) methylates histone H3 lysine 27 (H3K27me) and this histone post-translational modification (PTM) is associated with transcriptional repression. PRC2 requires three core subunits for minimal H3K27-directed methyltransferase activity (SUZ12, EED, and EZH2), while a fourth subunit, RbAp46/48, and other accessory proteins further enhance PRC2 methyltransferase activity.[4] In the hierarchical model of Polycomb recruitment, PRC2 binds to chromatin and the methyltransferase subunit EZH2 mediates the trimethylation of H3K27 (Figure 1A). Importantly, Embryonic Ectoderm Development (EED) binds the H3K27me3 mark deposited by EZH2, which ensures the propagation of H3K27me3 on adjacent nucleosomes via allosteric activation of EZH2 catalytic activity.[5] Specifically, EED recognition of H3K27me3 results in stabilization of the

Received: December 20, 2019
Published: April 29, 2020

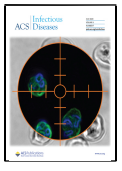

https://dx.doi.org/10.1021/acsinfecdis.9b00514
ACS Infect. Dis. 2020, 6, 1719−1733

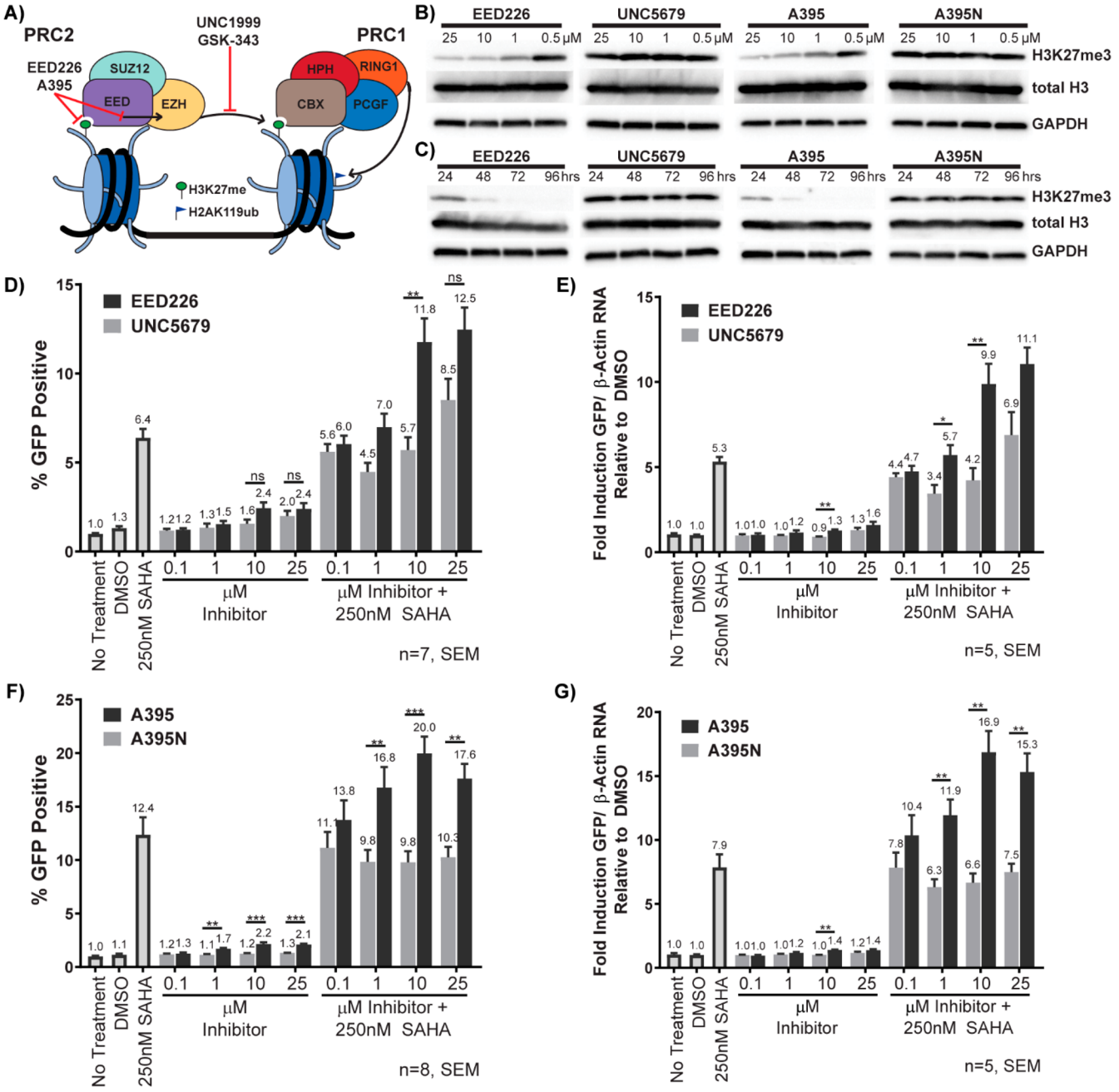

Figure 1. EED inhibitors reactivate latent HIV in 2D10 cells. (A) Core components of PCR2 and PRC1 and small molecule inhibitors used in this study. (B) 2D10 cells were treated for 72 h with various concentrations of EED226 and A-395, resulting in a dose dependent decrease in H3K27me3 as compared to controls UNC5679 and A-395N. (C) 2D10 cells were treated with 10 μM EED226, A-395, or controls for the time points indicated to determine optimal reduction of H3K27me3 levels. A 72-h treatment of 2D10 cells with EED inhibitors EED226 (D) and A-395 (F) with and without the addition of HDAC inhibitor SAHA (Vorinostat, 250 nM) for the final 24 h show increased HIV latency reactivation as measured by GFP expression via flow cytometry and GFP RNA level (E,G) relative to controls UNC5679 and A-395N respectively. (*$p < 0.05$, **$p < 0.01$, ***$p < 0.001$, Mann–Whitney Test).

stimulation responsive motif (SRM) of EZH2 which in turn stabilizes the SET domain of EZH2 for catalysis.[6] The subsequent recognition of H3K27me3 by Polycomb Repressive Complex 1 (PRC1) then blocks gene activation by catalyzing monoubiquitination of H2A on K119 (H2AK119ub1) through its RING1 E3 ligases, thus establishing a feed-forward mechanism of gene silencing. However, the relationship between PRC1 and PRC2 may be far more complex, with recent findings pointing to an alternative model in which the traditional roles of PRC1 and PRC2 are exchanged, whereby PRC1 initiates gene silencing via placement of H2AK119ub1 independently of H3K27me3 and subsequently recruits PRC2.[7−9]

The presence of both H3K27me3 and EZH2 at the HIV promoter in cell culture and primary cell models of latency[10−14] suggest that transcriptional repression by PRC2 plays a key role at the HIV long terminal repeat (LTR) promoter. Both shRNA-mediated knockdown of EZH2 and the use of EZH2-selective inhibitors promote latency reversal and synergize with other known LRAs including TNFα,

https://dx.doi.org/10.1021/acsinfecdis.9b00514
ACS Infect. Dis. 2020, 6, 1719−1733

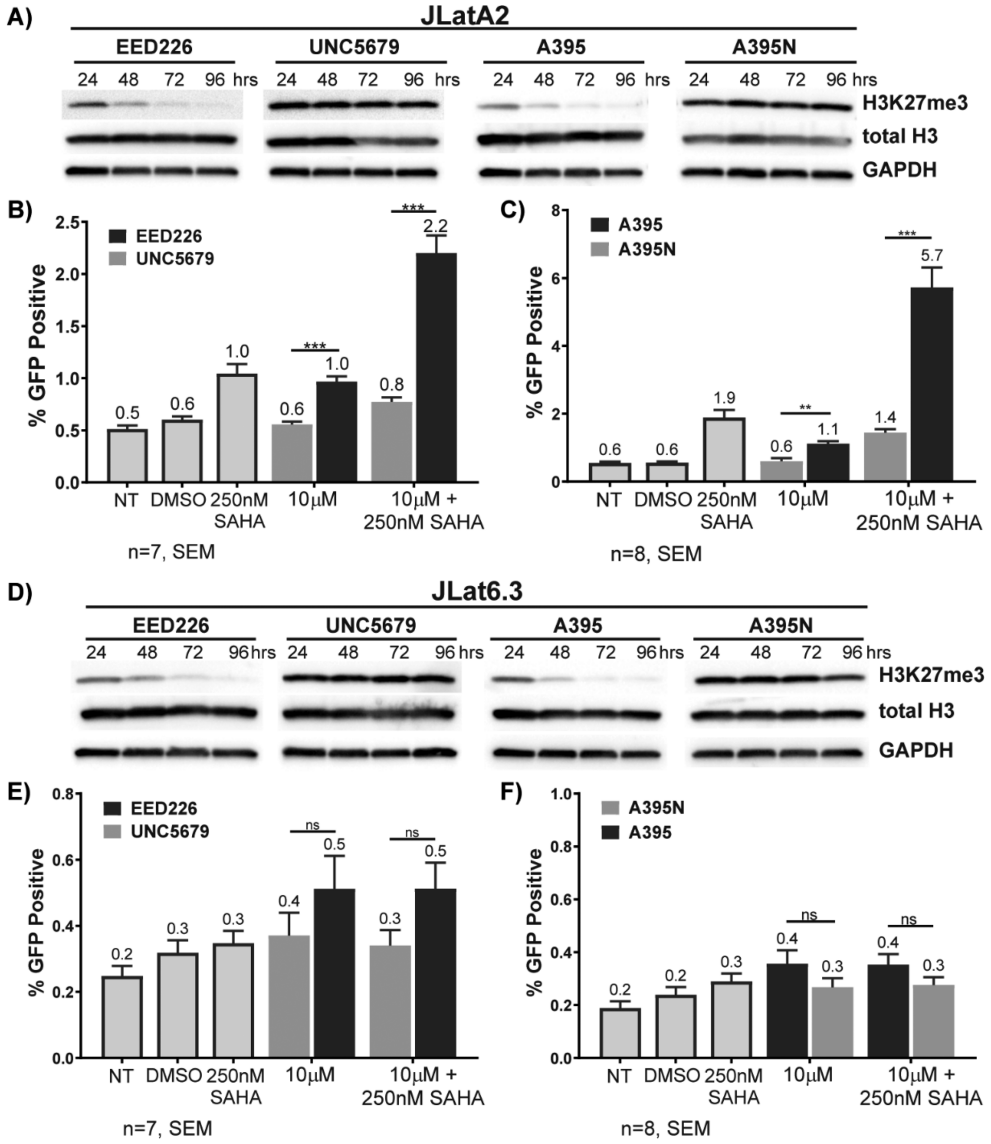

Figure 2. EED inhibitors reactivate latent HIV in JLatA2 Jurkat cells but not JLat6.3 cells. EED inhibitors EED226 and A-395 reduce global H3K27me3 in JLatA2 cells (A) and demonstrate latency reversal at 10 μM doses with and without 250 nM SAHA as measured by GFP expression (B,C). Meanwhile, JLat6.3 cells are unresponsive to EED inhibitors (E,F) despite equivalent reductions in global H3K27me3 (D) (*p < 0.05, **p < 0.01, ***p < 0.001, Mann−Whitney Test).

SAHA, and JQ1.[10,12] This strongly suggests that EZH2 is active in the maintenance of HIV latency, and that loss of H3K27me3 primes the LTR for reactivation. While EZH2 inhibitors (EZH2i) continue to be actively studied as potential LRAs, modulation of other PRC2 components and recruitment mechanisms for latency reversal has been less well explored to date. Two potent small molecule inhibitors of the PRC2 methyl-lysine reader EED were recently reported. A-395[15] and EED226[16] are chemically distinct yet they both interact with the 7-blade β-propeller WD40 domain of EED and inhibit recognition of H3K27me3 as well as the ability of EED to allosterically activate EZH2, resulting in abrogation of PRC2 methyltransferase activity and global loss of H3K27me3 in cancer cell models. As such, we sought to determine if EED inhibitors (EEDi) could modulate HIV latency similarly to EZH2 inhibitors (EZH2i).[12] Herein we demonstrate that both EED226 and A-395 can successfully reactivate latent HIV proviruses and therefore act as bona fide LRAs, representing a new class of PRC2-targeted molecules for use in HIV cure strategies.

RESULTS

EED Inhibitors Facilitate Latency Reactivation in 2D10 Cells. To examine the ability of EED inhibitors to act as LRAs, we first utilized 2D10 cells, a Jurkat-derived model which expresses GFP upon reactivation of the LTR.[11,12] After a 72 h treatment with varying concentrations of EED226 or A-395, we observed that a 10 μM dose, which is a concentration consistent with prior published observations of cellular activity for both compounds,[15,16] effectively reduced global H3K27me3 levels as compared to their structurally similar negative control compounds, A-395N and UNC5679, respectively (Figure 1B). A subsequent time course study confirmed near complete loss of H3K27me3 72 h after treatment with 10 μM EEDi and as such we used this time

https://dx.doi.org/10.1021/acsinfecdis.9b00514
ACS Infect. Dis. 2020, 6, 1719−1733

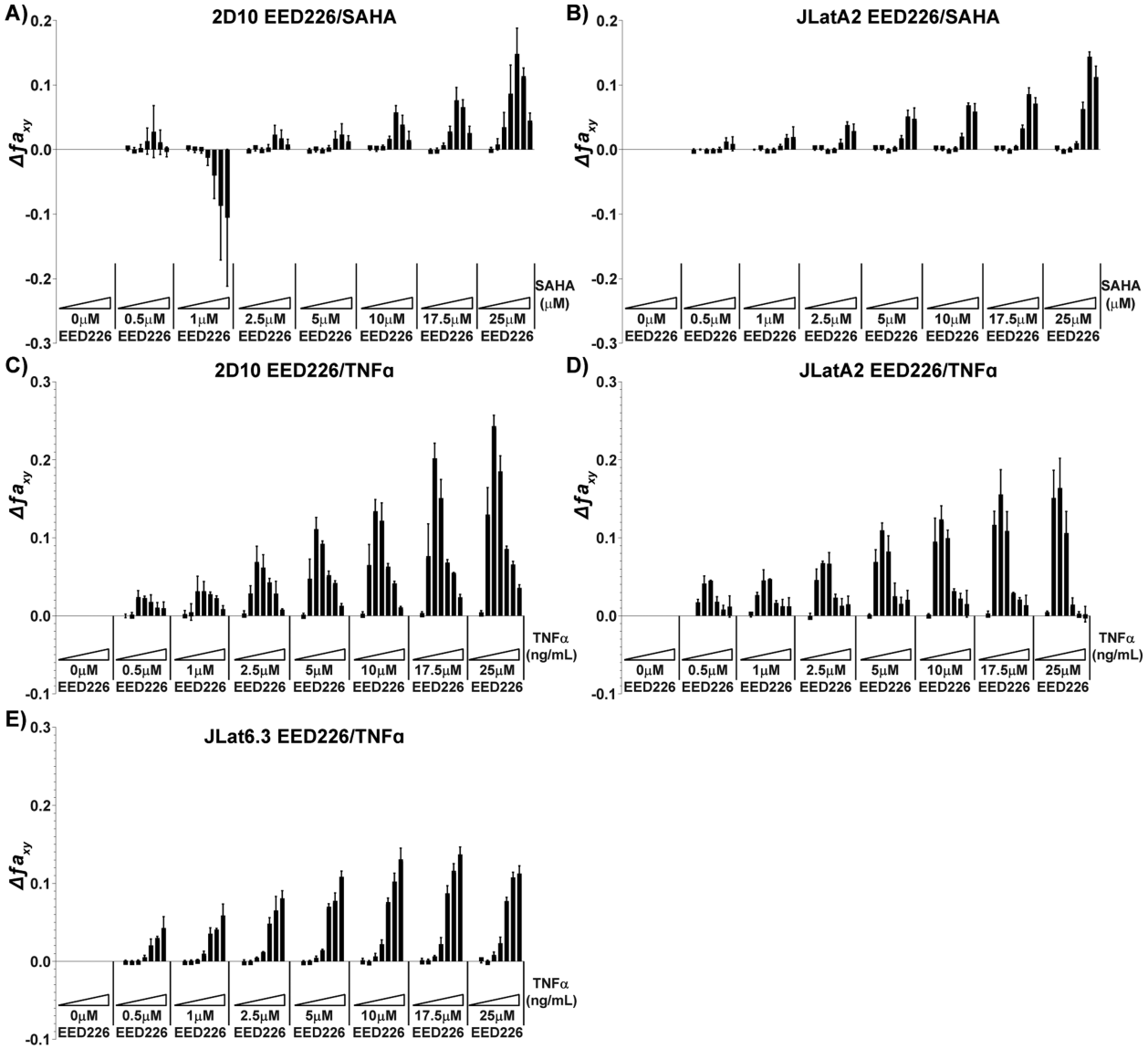

Figure 3. EED226 demonstrates Bliss Synergy with SAHA and TNF. Eight-concentration titrations of EED226 with SAHA (n = 6, SEM) in (A) 2D10 and (B) JLatA2 cells or with TNFα (n = 2, range) in (C) 2D10, (D) JLatA2, and (E) JLat6.3 cells display synergistic latency reactivation as determined by the Bliss Independence Model.

point to test for latency reactivation in Jurkat cells in all additional experiments (Figure 1C).

We then treated 2D10 cells with varying doses of A-395 or EED226 and evaluated the effect on HIV LTR activation. Cells were treated with EEDi or controls for a total of 72 h at 0.1, 1, 10, and 25 μM with minimal impact on viability (Supplemental Figure S1A). The response to 10 μM EED226 alone in 2D10 cells was modest but reproducible, inducing a 1.8-fold increase in GFP expression over DMSO treatment as determined by flow cytometry but failed to achieve significance over the equivalent UNC5679 treatment (Figure 1D, n = 7). However, UNC5679 has a reported IC_{50} of 20 μM for EED, and hence it was not surprising to observe a small amount of activity with this control compound at the top concentration tested.[17] Quantitative real-time PCR (qPCR) analysis of GFP transcript levels from cells treated with various concentrations of EED226 demonstrated a statistically significant increase at 10 μM over the UNC5679 control (Figure 1E, $p < 0.01$, n = 5).

To further confirm that the observed effect was on target and that EED inhibition results in reactivation, we treated 2D10 cells with A-395 in a similar fashion. Treatment with 10 μM A-395 resulted in a very similar, modest 1.9-fold increase in GFP protein expression over the DMSO control (Figure 1F, $p < 0.001$ for n = 8). A-395-induced LTR activation was significant at 1, 10, and 25 μM as compared to A-395N which had no effect at any of the concentrations tested (Figure 1F). qPCR analysis of GFP transcript levels additionally showed a significant increase in GFP expression upon treatment with 10 μM A-395 relative to A-395N (Figure 1G).

Recent studies posit that combination LRAs may be necessary to modulate sufficient reactivation to clear the latent reservoir.[18] We therefore tested both EEDi in combination with the histone deacetylase (HDAC) inhibitor suberoylanilide hydroxamic acid (SAHA, Vorinostat), one of the most well characterized and clinically advanced LRAs.[19−21] To do this, cells were treated with varying concentrations of EEDi for 72 h with the addition of a suboptimal concentration of SAHA (250

https://dx.doi.org/10.1021/acsinfecdis.9b00514
ACS Infect. Dis. 2020, 6, 1719−1733

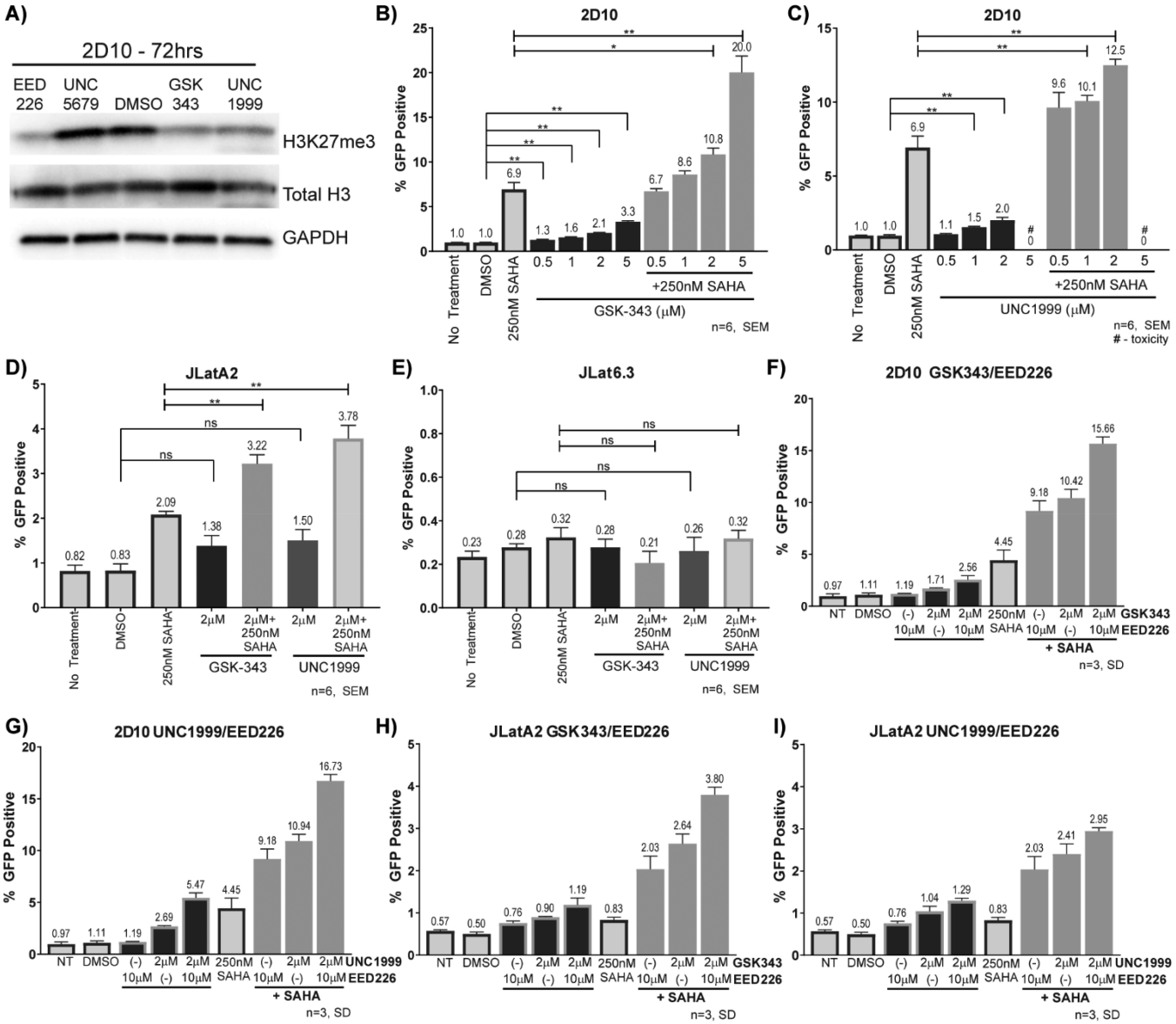

Figure 4. EED inhibitors phenocopy EZH2 inhibitors. (A) A 72 h treatment of EZH2 inhibitors UNC1999 (2 μM) and GSK343 (5 μM) decreases global levels of H3K27me3 to a similar degree as 10 μM EED226. A 72 h treatment of varying concentrations of EZH2 inhibitors GSK343 (B) and UNC1999 (C) with and without HDAC inhibitor SAHA (250 nM) for the final 24 h reactivate 2D10 cells to comparable levels as EED inhibitors. JLatA2 (D) and JLat6.3 (E) cells respond similarly to EZH2 inhibitors as EEDi, whereby EZH2 inhibitors can induce latency reactivation in JLatA2 cells but not JLat6.3 cells. Treatment of GSK343 (F,H) or UNC1999 (G,I) in combination with EED226 increases latency reactivation in 2D10 and JLatA2 cells as compared to individual compounds alone. In triple combination studies with SAHA, HIV LTR reactivation further increases over EEDi/SAHA and EZH2i/SAHA double combinations (*p < 0.05, **p < 0.01, ***p < 0.001, Mann−Whitney Test).

nM) for the last 24 h. In 2D10 cells, treatment with 250 nM SAHA alone averaged a 4.9-fold (Figure 1D) and 10.7-fold (Figure 1F) induction in GFP expression over DMSO when treated in parallel with EED226 and A-395, respectively. When combined with 10 μM EEDi, induction of GFP expression increased to 9-fold for EED226 and 17.3-fold for A-395 relative to the DMSO control, nearly doubling the response to SAHA alone in each case. Importantly, a similar increase in reactivation was not observed in the combination experiments including SAHA and the corresponding negative control compounds. GFP RNA levels also increased significantly in these combination studies with EED226 or A-395 and SAHA, as expected (Figure 1E and 1G). It should be noted that EED226 and A-395 were evaluated at separate times and with different stocks of SAHA and cells, resulting in a differential baseline of SAHA induction; however, the reactivation trends remain similar between both compounds when considering the fold induction over the SAHA baseline.

Latency Reactivation by EED Inhibitors Is Model-Dependent. Numerous Jurkat-derived models of latency which express GFP upon activation of the HIV LTR exist and are commonly used in laboratories to assess LRAs. We chose to extend our studies to two additional cell lines, the JLatA2 and JLat6.3 models,[22,23] to minimize bias which could be observed by only testing in a single latency model.[24] In addition, these lines harbor different reporter constructs[11,22,23] and likely have differing integration sites, although only the 2D10 line has been characterized.[11] As compared to 2D10 cells, the JLatA2 and JLat6.3 cell lines demonstrate differential responses to commonly used LRAs such as tumor necrosis

https://dx.doi.org/10.1021/acsinfecdis.9b00514
ACS Infect. Dis. 2020, 6, 1719−1733

factor alpha (TNFα), SAHA, and PMA/Ionomycin (Supplemental Figure S2) as measured by GFP expression via flow cytometry. The JLatA2 line is slightly less responsive to both TFAα and SAHA than the 2D10 cells, while the JLat6.3 line is weakly responsive to all three LRAs.

We first sought to confirm that EEDi reduces H3K27me3 levels in these additional latency models. As expected, in both the JLatA2 and JLat6.3 models, treatment with 10 μM EED226 or A-395 over a period of 96 h resulted in a decrease in global H3K27me3 levels (Figure 2A and 2D). However, when tested for changes in GFP expression in response to EEDi treatment, latency reactivation was only observed in the JLatA2 cells and not the JLat6.3 cells, despite the ability of both EED inhibitors to impact global H3K27me3 levels (Figure 2 and Supplemental Figures S3 and S4). Like in 2D10 cells, treatment with 10 μM EED226 alone in JLatA2 cells resulted in a modest effect, inducing a 1.6-fold (Figure 2B, $p < 0.001$ for $n = 7$) increase in GFP protein expression as compared to the DMSO control (Figure 2B, $p < 0.001$ for $n = 7$) while 10 μM A-395 induced a 2-fold increase (Figure 2C, $p < 0.01$ for $n = 8$). In combination with 250 nM SAHA, both EEDi resulted in significant 3- to 4-fold increases in reactivation relative to SAHA alone at 10 μM. Additionally, the extent of reactivation upon treatment with 1 and 25 μM EEDi in combination with SAHA was determined to be significant (Figures 2B and 2C, Supplemental Figures S3A and S4A). Significant induction of GFP mRNA was also observed in JLatA2 cells in response to both EEDi at 10 and 25 μM, and at 1, 10, and 25 μM in combination with SAHA (Supplemental Figures S3A and S4A).

In contrast, the JLat6.3 line did not respond to either EED inhibitor alone at any concentration or in combination with 250 nM SAHA as measured by protein or RNA expression (Figure 2E and 2F, Supplemental Figures S3B and S4B). The lack of activity in the JLat6.3 cell line was not wholly unexpected, as in our hands this line does not respond to HDAC inhibitors (Figure 2E and 2F) and reactivates only weakly in response other robust LRAs such as TNFa and mitogen PHA (Supplemental Figure S2). Overall, these results demonstrate that EEDi mediate modest increases in GFP protein and HIV mRNA expression alone, and significantly higher increases in combination with SAHA in certain cell models of latency, further supporting the notion that combinations of LRAs may be required to increase proviral expression in a meaningful way.

EED226/SAHA Combinations Demonstrate Bliss Synergy. Our observation that treatment with EED226 and A-395 in combination with SAHA doubled latency reactivation as compared to SAHA alone suggested potential synergy between EEDi and SAHA. To further examine this, we performed an 8-point titration of EED226 with increasing concentrations of SAHA in both 2D10 and JLatA2 cells. We used the Bliss Independence Model to analyze the data which determines if multiple compounds, when used in combination, display antagonism ($\Delta fa_{xy} < 0$), are independent ($\Delta fa_{xy} = 0$), or are synergistic ($\Delta fa_{xy} > 0$). Consistent with our earlier observations, we observed an overall synergistic relationship between EED226 and SAHA in both cell types (Figure 3A and 3B). We observed some antagonism in 2D10 cells with low doses of EED226 (1 μM); however, this was not observed in JLatA2 cells.

We further tested EED226 all three Jurkat latency models in combination with TNFα, a strong activator of the NF-κB pathway. Consistent with the ability of TNFα to maximally activate the proviral reporter in both 2D10 and JLatA2 cells (Supplemental Figure S2), we saw the most synergy with EED226 at concentrations ranging from 0.1 to 1 ng/mL of TNFα, above which any synergy declined due to maximal stimulation by TNFα (Figure 3C and 3D). Most notably, we observed increasing synergy in JLat6.3 cells up to the highest concentration of TNFα (Figure 3E). This observation suggests that while no LRA activity is observed by EEDi alone in JLat6.3 cells, there is still a role for this epigenetic restriction and that EEDi can be combined with highly potent LRAs to more effectively induce transcription from highly repressed proviruses in these Jurkat models.

EED Inhibitors Phenocopy EZH2 Inhibitors in Cellular Models of Latency. As EED226 and A-395 demonstrated overall comparable LRA activity in all Jurkat lines, we moved forward with additional characterization of latency reversal with EED226 due to more favorable pharmacokinetics via oral administration as compared to A-395.[15,16] We compared the extent of latency reversal with EED226 to that of two well-characterized EZH2 inhibitors, GSK343[25] and UNC1999,[26] both which bind to the EZH2 SET domain and inhibit EZH2 catalytic activity. First, we observed that EED226, GSK343, and UNC1999 treatment of 2D10 cells for 72 h resulted in comparable decreases in global H3K27me3 levels by Western blot (Figure 4A). Subsequent treatment of 2D10 cells with 2 μM GSK343 or UNC1999 showed a 2.1-fold and 2.0-fold increase in GFP expression over DMSO, respectively (Figure 4B and 4C). Treatment of 2D10 cells with 250 nM SAHA alone showed a 6.9-fold increase in GFP expression over DMSO; however, upon combination with GSK343 and UNC1999, GFP expression increased further to 10.8-fold and 12.5-fold, respectively, over DMSO (Figure 4B and 4C). In JLatA2 cells, more modest effects were observed, as expected. Treatment of JLatA2 cells with 2 μM GSK343 did not induce a significant increase in GFP expression over DMSO while 2 μM UNC1999 induced a 1.8-fold increase ($p < 0.05$) (Figure 4D). In combination with SAHA, 2 μM GSK343 resulted in a 3.9-fold increase and UNC1999 a 4.5-fold increase in GFP expression over DMSO while SAHA alone induced a 2.5-fold increase (Figure 4D, Supplemental Figure S5A). Overall, in both 2D10 and JLatA2 cells, the combination of EZH2i with SAHA increased HIV reactivation approximately 2-fold over SAHA alone. Importantly, these results closely parallel those with EEDi and demonstrate the ability of EEDi to phenocopy EZH2i in these models. Consistent with our observations using EED inhibitors, neither EZH2 inhibitor mediated a significant increase in GFP expression alone or in combination with SAHA in JLat6.3 cells (Figure 4E, Supplemental Figure S5B). We found that both GSK343 and UNC1999 demonstrated signs of toxicity at 5 μM as measured by a viability dye stain, decreasing viability by 10% and over 50%, respectively (Supplemental Figure S5C–E). Consequently, we proceeded to use lower doses of EZH2i in future experiments as GFP expression may also be induced at this concentration due to cell stress.

EEDi and EZH2i Combination Treatments Enhance Viral Reactivation in Jurkat Latency Models. We next tested EED226 in combination with both GSK343 and UNC1999. While mechanistically both EEDi and EZH2i function by reducing PRC2 catalytic activity and H3K27me3-mediated repression, we sought to determine if dual treatment would be more effective at reserving latency relative to the individual inhibitors. Encouragingly, combination treatments

https://dx.doi.org/10.1021/acsinfecdis.9b00514
ACS Infect. Dis. 2020, 6, 1719−1733

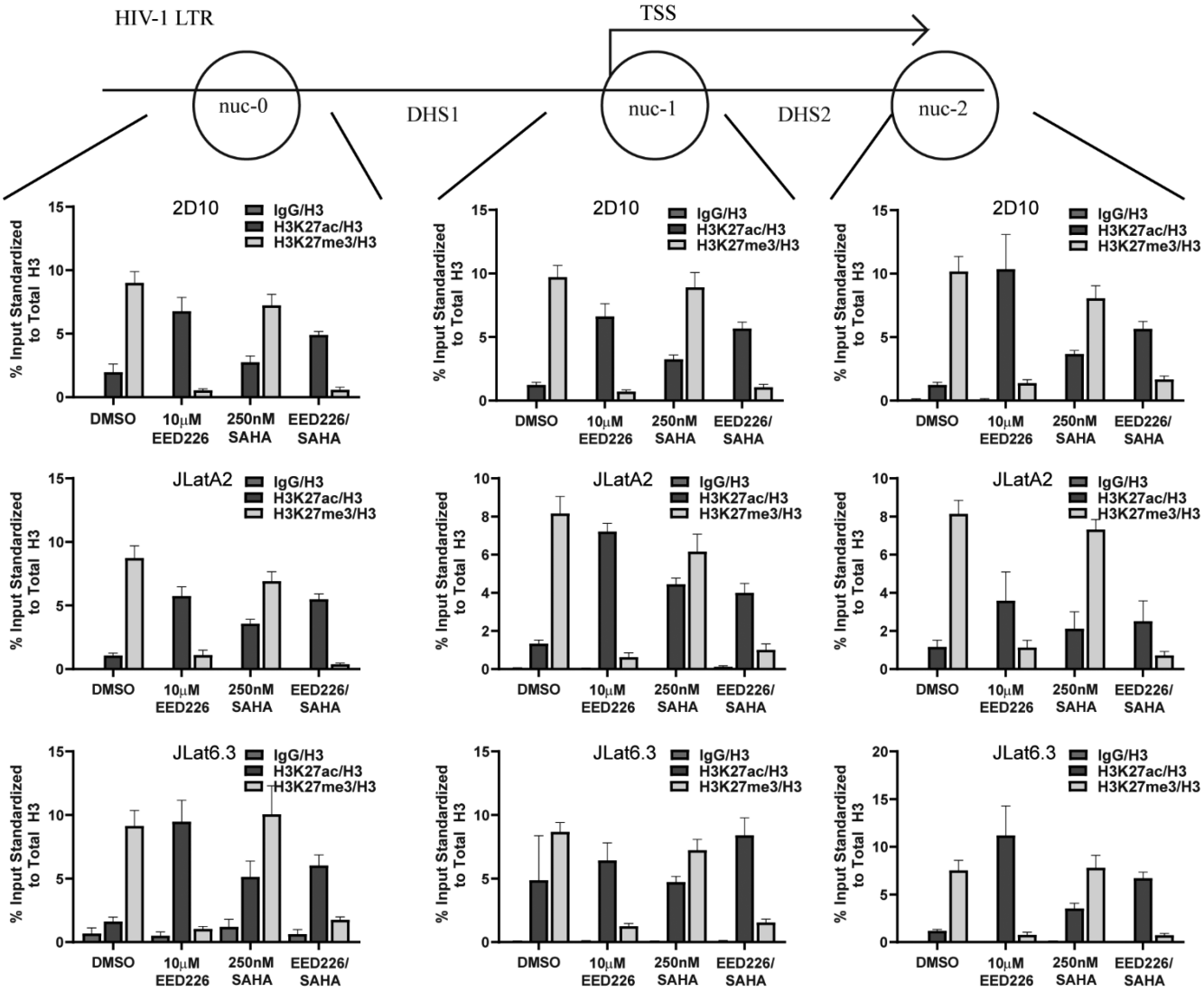

Figure 5. EED226 can toggle H3K27 methylation and acetylation at the HIV LTR. Chromatin immunoprecipitations demonstrate that EED226 treatment (10 μM) results in a decrease in H3K27me3 and a corresponding increase in H3K27ac at the HIV LTR at all three canonical nucleosomes. SAHA treatment alone does not result in a strong shift in H3K27 modifications. Error bars represent n = 6, SEM.

of EED226 with either GSK343 or UNC1999 for 72 h resulted in an increase in GFP expression over the treatment with EED226 alone. When EED226 (10 μM) was combined with GSK343 (2 μM), induction of GFP expression increased 2.3-fold over DMSO (Figure 4F) compared to 1.5-fold induction with GSK343 alone in 2D10 cells. Meanwhile, treatment with EED226 (10 μM) and UNC1999 (2 μM) increased GFP expression 4.9-fold over the DMSO control in 2D10 cells, which is the strongest LRA activity observed with any PRC2i, while single inhibitor treatment either showed no increase over DMSO (EED226) or a 2.4-fold increase (UNC1999) (Figure 4G). Comparable experiments in JLatA2 cells demonstrated similar trends (Figure 4H and 4I). Due to the fact that increased latency reversal activity was observed with simultaneous treatment of PRC2 inhibitors targeting different components of the complex, we next performed triple-combination experiments with SAHA as described previously. We observed a 3.5-fold (EED226/GSK343/SAHA, Figure 4F) and 3.7-fold (EED226/UNC1999/SAHA, Figure 4G) increase in reactivation in 2D10 cells over SAHA alone, and 4.6-fold (EED226/GSK343/SAHA, Figure 4H) and 3.5-fold (EED226/UNC1999/SAHA, Figure 4I) increase over SAHA alone in JLatA2 cells. Overall, combination EEDi/EZH2i treatments resulted in small yet consistent increases in GFP expression across multiple cell lines, likely due to a more complete inhibition of PRC2 in these model systems. As expected, the addition of SAHA resulted in a more significant boost in GFP expression; however, the overall reactivation of combination EEDi/EZH2i/SAHA treatments did not result in appreciably higher levels of GFP expression than previously observed with a single PRC2 inhibitor and SAHA.

Reciprocal Regulation of H3K27me3 and H3K27ac Globally and at the HIV-LTR. Although inhibition of EED reduces H3K27me3 levels globally in our cellular models, it was unclear if EED inhibition directly affected the levels of H3K27 methylation at the HIV LTR. To address this, we performed MNase chromatin immunoprecipitation (MNase ChIP) for H3K27me3 and H3K27ac in all three Jurkat latency models before and after EED226 treatment. We observed a substantial loss of H3K27me3 at the LTR upon treatment with EED226 (Figure 5). Interestingly, we also observed that loss of H3K27me3 resulted in a concomitant increase in H3K27ac—

https://dx.doi.org/10.1021/acsinfecdis.9b00514
ACS Infect. Dis. 2020, 6, 1719−1733

an active chromatin mark—both at the HIV LTR and globally. While H3K27ac was detectable in untreated cells at a range of 0.5−2% of input depending on the nucleosome and cell line assessed, H3K27ac increased to 6−10% of input after treatment with EED226 (Figure 5). Meanwhile, H3K27me3 levels ranged from 7 to 12% of input prior to EED226 treatment, which decreased to less than 2% of input upon treatment with EED226 (Figure 5). In comparison, treatment with 250 nM SAHA alone resulted in an increase in H3K27ac in some cases, yet H3K27me3 was consistently present at higher levels than H3K27ac. Overall, combination treatments of EED226 with SAHA closely resembled EED226 treatment alone (Figure 5). To determine whether other H3 modifications were similarly affected by EED inhibition, we evaluated the global levels of H3K9me3, H3K9ac, and H3K4me3 (Figure 6). In each case, EED226 treatment did not appear to impact levels of these other relevant histone post-translational modifications on a global level.

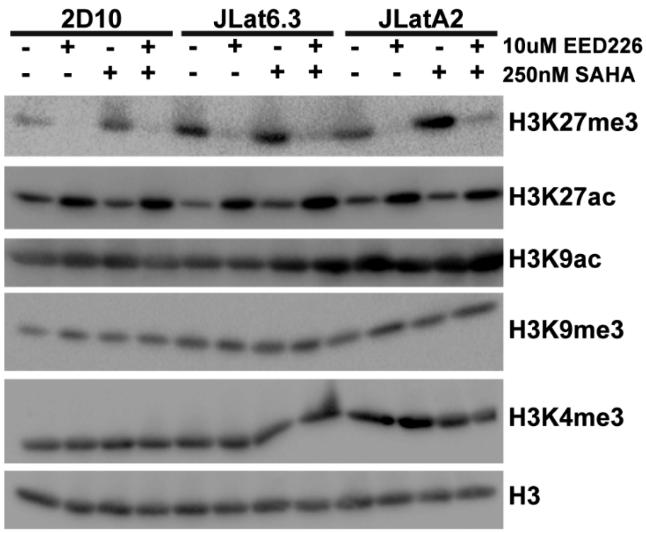

Figure 6. EED226 treatment alters H3K27me3 and H3K27ac levels globally. Analysis of 5 histone modifications on a global level demonstrates only H3K27 marks are impacted by EED226 treatment while H3K9me3, H3K9ac, and H3K4me3 are unchanged.

Global H3K27me3 Levels Are Not Significantly Reduced by PRC2i in Primary CD4+ T-Cells. Given that PRC2 inhibition resulted in decreased H3K27me3 levels and showed significant promise in reactivating latency in Jurkat cell lines, we next sought to determine if similar effects would be observed in primary CD4+ T-cells. We examined global H3K27me3 levels in total CD4+ T-cells isolated from healthy donors upon treatment of single doses of both EEDi (A-395 and EED226) and EZH2i (UNC1999 and GSK343) after 72 and 96 h. In each case, we observed no change in global H3K27me3 levels (Figure 7A and 7B). To explore this further, we assayed additional doses of both EEDi and EZH2i and time points (24, 48, and 72 h). Consistent with our initial results, we observed no significant decrease in global H3K27me3 levels in total CD4+ T-cells at any time point or dose of PRC2i in two independent donors (Figure 7C and Supplemental Figure S6A). This was observed with both EED and EZH2 inhibitors, the latter of which have been previously shown to modulate latency reversal in primary cell models.[12,14] Quantitation of H3K27me3 levels standardized to total histone H3 showed both decreasing and increasing changes relative to the untreated control (Figures 7D and E, Supplemental Figure S6B,C); however, there do not appear to be any consistent trends and the changes observed are far less substantial than those seen in the Jurkat models.

We further assessed the tolerability of both EEDi and EZH2i in donor cells by examining activation markers CD25 and CD69 as well as cellular viability via an alamarBlue assay. In total CD4+ T-cells isolated from 5 healthy donors, we observed no significant toxicity at 72 or 96 h after treatment with EED226 (up to 20 μM), A-395 (up to 20 μM), or GSK-343 (up to 5 μM), while we observed a minor decrease in viability at 5 μM UNC1999 (Figure 8A and 8B), consistent with toxicity at this dose of UNC1999 in Jurkat cells. We observed no major change in the expression of either CD69 or CD25 in treated cells at 72 (Figure 8C) or 96 h (Figure 8D), although a slight trend toward activation in 5 μM UNC1999 treated cells was observed which is consistent with the toxicity data. Overall, this demonstrates that treatment of donor cells with EEDi does not affect cell viability at the doses utilized.

DISCUSSION

The use of LRAs in strategies to clear persistent HIV infection seeks to induce expression of quiescent HIV to a level detectable by immune clearance mechanisms.[1] Reversal of HIV latency has focused on the two main mechanisms of transcriptional repression, restriction of critical host factors and epigenetic repression of the integrated provirus. While there is a significant understanding of the former[27] in the role of HIV transcription and latency, there is still work to be done in understanding the full impact of the latter.[28]

The Polycomb Repressive Complexes, PRC1 and PRC2, are critical regulators of gene silencing through the installation and recognition of the repressive H3K27me3 PTM, and hence are likely to make a significant contribution to HIV latency. Here we demonstrate that a new class of PRC2 inhibitors which target the methyl-lysine reader protein EED can induce latency reversal in model systems, resulting in similar levels of reactivation to that of EZH2 inhibitors. These EED inhibitors demonstrated limited toxicity in Jurkat latency models and resulted in both a global decrease in the repressive H3K27me3 mark and an increase in the activating H3K27ac mark. This reciprocal relationship between H3K27me3 and H3K27ac has previously been observed in mouse embryonic stem cells, where EED, EZH2, or SUZ12 knockout resulted in increased H3K27ac levels, further suggesting a direct link to PRC2.[29] More recent work has reproduced these observations using EZH2 and EED small molecule inhibitors, and the histone acetyltransferases p300 and CBP have been implicated in the upregulation of H3K27ac.[29,30] Interestingly, the role of p300/CBP in initial LTR activation is well-established.[31−33]

While modulation of PRC2 activity alone resulted in limited HIV reactivation, the combination of EEDi with the HDAC inhibitor SAHA significantly improved overall latency reactivation in 2D10 and JLatA2 cells as compared to either agent alone. This reinforces the idea that multiple histone marks may act to layer repressive signals, each of which needs to be removed in order to promote sufficient transcription of the HIV provirus to produce detectable antigen for latency clearance strategies. Other studies using single epigenetic agents have shown latency reversal in only a minority of proviruses within primary cells obtained from HIV-infected donors.[34] In contrast to the 2D10 and JLatA2 cells, the JLat6.3

https://dx.doi.org/10.1021/acsinfecdis.9b00514
ACS Infect. Dis. 2020, 6, 1719−1733

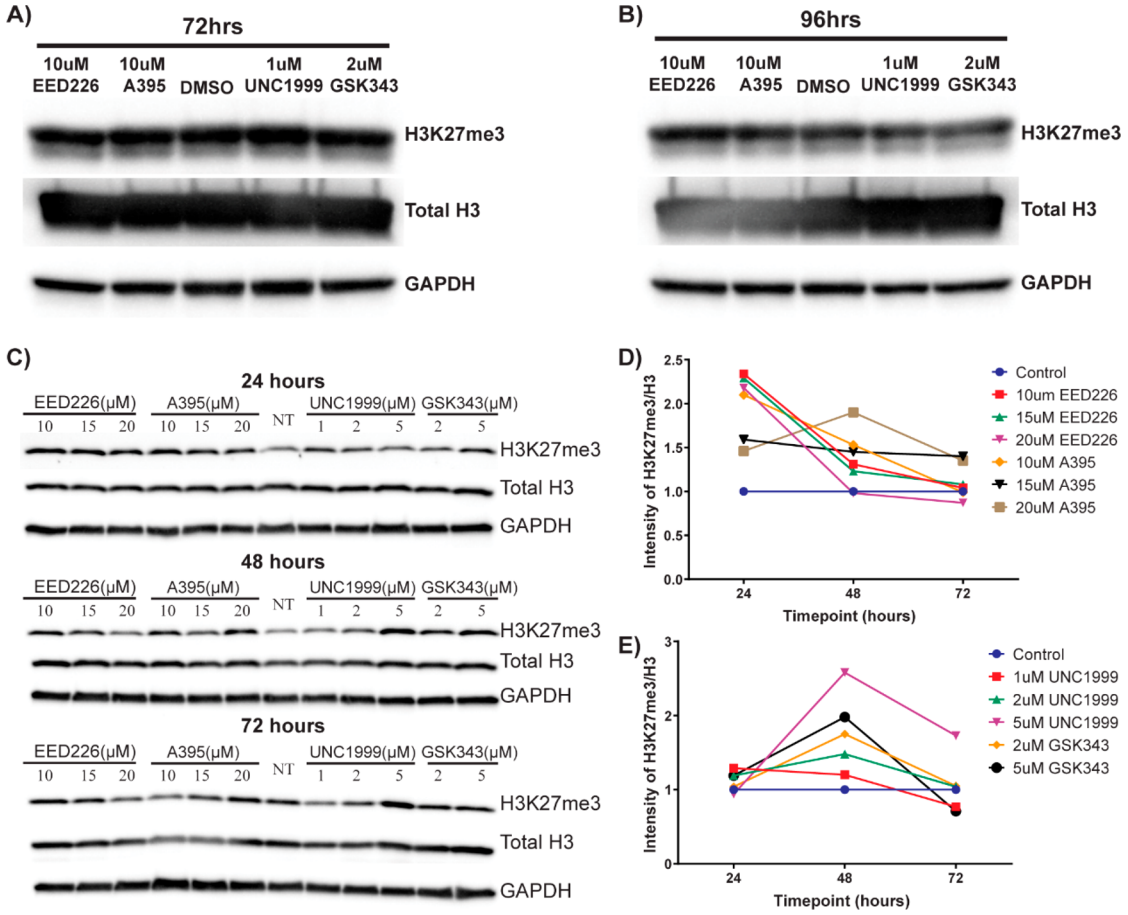

Figure 7. Effects of EEDi and EZH2i on H3K27me3 levels in primary CD4+ T-cells. Initial assessment of the impact of EEDi and EZH2i on H3K27me3 levels in total CD4+ T-cells at (A) 72 and (B) 96 h shows no decrease in H3K27me3 levels. (C) Treatment of total CD4+ T-cells isolated from a healthy donor with extended concentrations of EEDi (A-395 and EED226) and EZH2i (UNC1999 and GSK343) for 24 to 72 h shows little to no change in global levels of H3K27me3. (D) Quantification of H3K27me3 levels from (C) standardized to total histone H3 levels for EEDi treatments. (E) Quantification of H3K27me3 levels from (C) standardized to total histone H3 levels for EZH2i treatments.

cell model was overall unresponsive to treatment with EEDi. The downregulation of H3K27me3 and increased H3K27ac was observed in all Jurkat models upon treatment with EEDi, suggesting that the lack of latency reversal observed with EED inhibitors (and other LRAs) in the JLat6.3 model is not necessarily due to lack of inhibitor activity, but instead the result of other confounding factors which impact LTR activation in these long-established models (e.g., integration site, presence of DNA methylation, and/or differential chromatin modifications). It has been previously reported that JLat6.3 cells show high levels of DNA methylation at the LTR,[35] a modification that is known to inhibit NF-kB binding and result in activation of HIV.[36,37] Indeed, we further observed synergy and an increase in the maximal reactivation achievable in JLat6.3 cells when EED226 was used in combination with TNFα, suggesting that, while not a dominant force, epigenetic restrictions exist in this model.

Our study of H3K27me3 levels in CD4+ cells upon treatment with PRC2 inhibitors strongly indicates that loss of H3K27me3 does not occur to the same extent as in Jurkat and other immortalized cell models. While it has previously been shown that the EZH2 inhibitor GSK343 can down-regulate H3K27me3 in total PMBCs,[12] this has not been demonstrated in isolated total CD4+ cells. The frequency of cells undergoing proliferation and high transcriptional activity is lower in peripheral CD4+ cells which have low basal levels of markers linked to activation.[38] The predominance of quiescent cells in the CD4+ cell populations studied would also not be expected to display turnover of H3K27me3 from histone exchange mediated by DNA replication or widespread gene transcription, further reducing the potential for PRC2 inhibitors to influence H3K27 methylation levels. We hypothesize that H3K27me3 loss is observed in Jurkat cells due to ongoing cell division, dilution of existing H3K27me3, and the inability of PRC2 to propagate the mark in the presence of inhibitors. In primary resting CD4+ T-cells, the lack of significant cell division may not allow for similar turnover, resulting in minimal changes in global H3K27me3 levels as compared to traditional cancer cell lines. This hypothesis is further supported by recent work demonstrating that replication dilution is a major path for the removal of H3K27 methylation.[39] These observations highlight potential difficulties associated with targeting the removal of repressive chromatin marks in the primary cell population most relevant to HIV latency reversal. Encouragingly, a recent study by Nguyen and colleagues using a highly sensitive next-generation sequencing-based assay demonstrated latency reversal in HIV+ donor memory CD4+ T-cells in response to EZH2 inhibitors alone and in combination with SAHA,[14] suggesting that PRC2 inhibitors have the potential to reactivate latency in patient cells and that a global downregulation of H3K27 methylation

https://dx.doi.org/10.1021/acsinfecdis.9b00514
ACS Infect. Dis. 2020, 6, 1719−1733

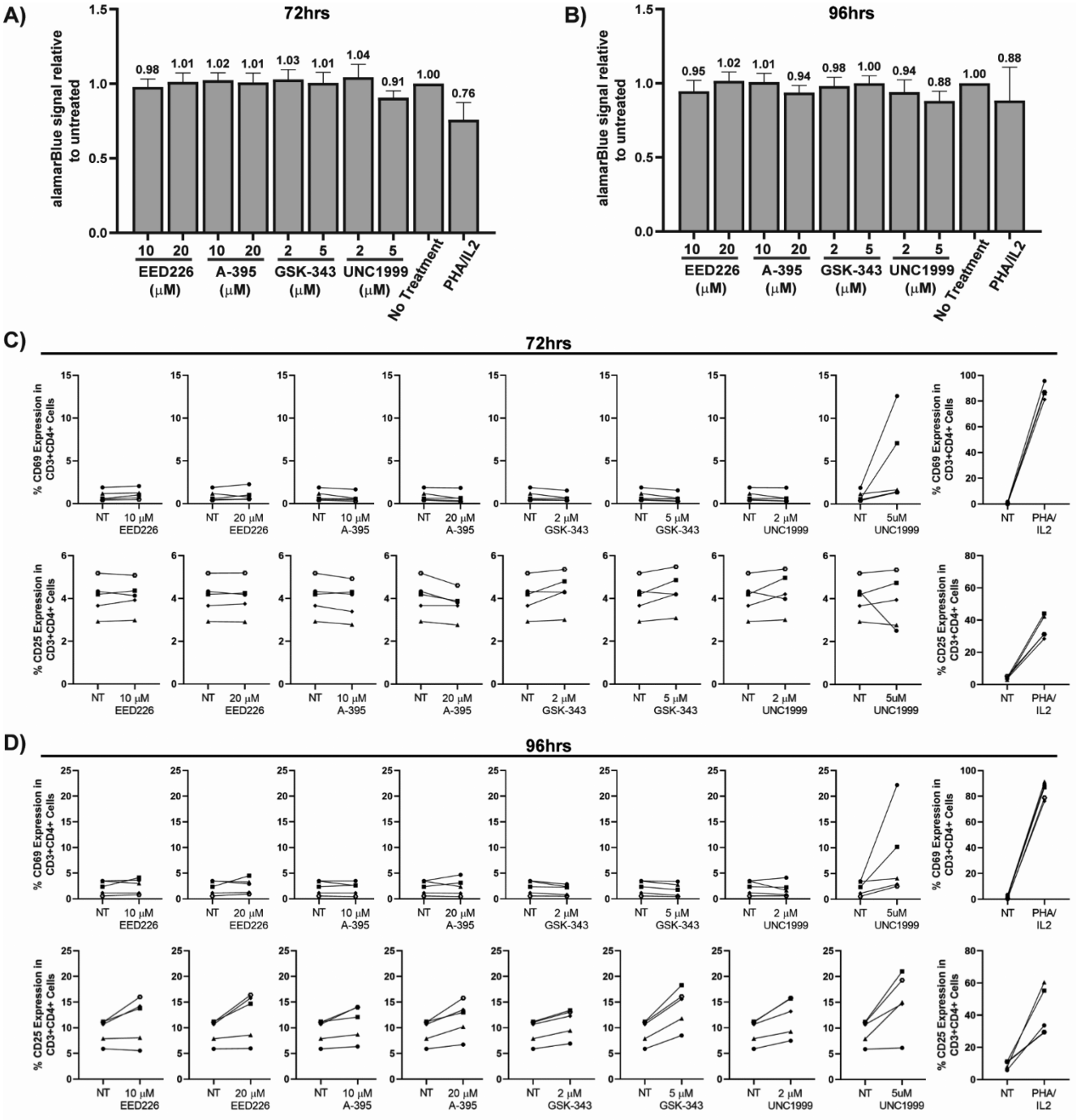

Figure 8. Tolerability of EEDi and EZH2i in primary CD4+ T-cells. To evaluate tolerability of EEDi and EZH2i in primary cells, alamarBlue was used to assay cellular viability after (A) 72 h or (B) 96 h of treatment in 5 donors. (C) CD69 and CD25 expression levels in tCD4+ T-cells from 5 healthy donors after treatment with EEDi or EZH2i for 72 h. (D) CD69 and CD25 expression levels in tCD4+ T-cells from 5 healthy donors after treatment with EEDi or EZH2i for 96 h.

in primary CD4+ T-cells may not be required for latency reversal in cells from HIV+ donors.

CONCLUSION

There is a significant body of prior work demonstrating a role for PRC2 in the maintenance of HIV latency and the potential for EZH2 inhibitors in latency reversal for cure strategies.[10−14] Here we add a new class of PRC2 inhibitors, EED inhibitors, to a growing list of agents to be considered for latency reversal studies. The identification of new targets for latency reversal and novel LRAs is likely to be critical as combination therapies are explored to maximally increase proviral expression. We demonstrate that EED inhibitors A-395 and EED226 phenocopy EZH2 inhibitors with regards to HIV latency reversal; however, EED inhibitors have the potential to be used without blocking PRC2-independent EZH2 activities,[40−42] are significantly less toxic in our in vitro models, and show no evidence of induction of activation markers in CD4+ T-cells. Furthermore, resistance to EZH2 inhibitors has been reported in cell culture,[43,44] potentially leading to clinical resistance to

https://dx.doi.org/10.1021/acsinfecdis.9b00514
ACS Infect. Dis. 2020, 6, 1719−1733

EZH2 inhibitors and providing a therapeutic advantage to blocking PRC2 activity with EED inhibitors. While our work suggests these LRAs may have limited function as single agents, EED and EZH2 inhibitors should continue to be considered for use in combination with other classes of LRAs to sensitize the HIV provirus to latency reactivation for HIV cure strategies. The evaluation of EEDi as LRAs in resting and total CD4+ T-cells isolated from antiretroviral therapy (ART) suppressed, aviremic individuals is the subject of ongoing work.

METHODS

Cell Lines. JLatA2 and JLat6.3[22,23] were obtained from the NIH AIDS Reagent Program. 2D10[11] cells were a gift from Dr. Jonathan Karn (Case Western Reserve). Cells were maintained in RPMI1640 (LifeTech) supplemented with 10% FBS (Millipore) and 100 U/mL Pen/Strep (LifeTech) at 37 °C/5% CO_2.

Inhibitors. A-395 (SML1923) and A-395N (SML1879) were purchased from Sigma-Aldrich. EED226 (HY-101117) was purchased from MedchemExpress. SAHA (S1047) was purchased from Selleckchem. Recombinant human TNF-alpha (210-TA-020) was purchased from R&D Systems. UNC5679 (*N*-(furan-2-ylmethyl)-8-phenylimidazo[1,2-*c*]pyrimidin-5-amine) was synthesized as previously reported[17] to yield the desired product as a white solid (6.6 mg) (see Supplemental Methods for additional information).

Latency Reversal/Flow Cytometry. Cells were plated in 96-well plates at 25 000/well and treated with inhibitors for indicated time periods. *N* indicates total number of biological replicates performed over three independent experiments. Half of cells were pelleted, flash frozen, and stored for later RNA isolation. The remaining half were stained with LIVE/DEAD Fixable Aqua Dead Cell Stain (ThermoFisher) for 30 min, followed by DPBS wash and fixation in 1.5% paraformaldehyde/DPBS. Cells were assayed using the iQue Screener Plus (Intellicyt) and GFP expression with dead-cell exclusion was calculated using the ForeCyt analysis software (Intellicyt).

Synergy. An 8-point cross titration of EED226 (0, 0.5, 1, 2.5, 5, 10, 17.5, and 25 μM) and SAHA (0, 0.0312, 0.0625, 0.125, 0.25, 0.5, 1, and 2 μM) or TNFα (0, 0.01, 0.1, 0.5, 1, 5, 10, and 100 ng/mL) was performed for an indicated number of replicates. EED226 was added for 72 h with SAHA or TNFα added at the indicated concentrations for the final 24 h to match conditions of prior experiments. Latency reversal was assayed via flow cytometry as described above. The Bliss Independence model[45] states that if two agents are independent in action, the predicted action of the two agents together ($fa_{xy,P}$) can be defined by the following: $fa_{xy,P} = fa_x + fa_y - (fa_x)(fa_y)$, where fa_x and fa_y are the observed action of the two drugs independent of each other. The experimentally observed action of the two in combination is represented as $fa_{xy,O}$. $\Delta fa_{xy} = fa_{xy,O} - fa_{xy,P}$, whereby $\Delta fa_{xy} < 0$ is antagonism, $\Delta fa_{xy} = 0$ is independence, and $\Delta fa_{xy} > 1$ is synergy. We calculated synergy similar to previously reported,[18,46] but omitted normalization to a positive control as none of our data was reported as such. For this work, fa(EED or SAHA/TNFα) = (Fraction GFP single agent − Fraction GFP DMSO) and $fa_{xy,O}$ = (Fraction GFP combo − Fraction GFP DMSO).

RNA/cDNA/qPCR Jurkats. Total RNA was isolated using the Quick RNA 96-well (Zymo) per manufacturer's instructions. cDNA was generated using the Maxima First Strand cDNA Synthesis Kit for RT-qPCR with dsDNase (ThermoFisher) per manufacturer's instructions. Gene expression was assayed by qRT-PCR using FastStart Universal SYBR Green Master (Roche) on the QuantStudio 5 (Applied Biosystems) with the following primer sets: GFP (F-5′ TCAAGATCCGCCACAACATC, R-5′ GTGCTCAGGTAGTGGTTGTC); β-Actin (F-5′ AGGTCATCACCATTGGCAATGAG, R-5′ TCTTTGCGGATGTCCACGTCA); GAPDH (F-5′ CAGGAGGCATTGCTGATGAT, R-5′ GAAGGCTGGGGCTCAT); TBP (F- 5′ GAGAGTTCTGGGATTGTACCG, R-5′ ATCCTCATGATTACCGCAGC). While GFP results standardized to β-Actin are presented here, GFP was also normalized to TBP and GAPDH and displayed similar increases in response to EEDi (data not shown).

Western Blots. Cells are lysed in a modified RIPA buffer (25 mM Tris-HCl pH 7.5, 150 mM NaCl, 1% Triton X-100, 0.5% sodium deoxycholate, 0.1% SDS, 1× complete protease inhibitor (Roche), 1X HALT Phosphatase inhibitor (ThermoFisher), 1 mM sodium butyrate, and 4 μL/mL Benzonase (Sigma) for 30 min on ice and cellular debris pelleted. Recovered supernatants are assayed for protein concentrations by the Detergent Compatible Bradford Assay (Pierce, ThermoFisher) according to manufacturer's instructions. Proteins are separated by 4−20% Tris-glycine acrylamide gel (TGX gels, BioRad) and transferred onto Immun-Blot PVDF membranes via semidry transfer using the Trans-Blot Turbo System (Bio-Rad). Membranes are blocked with tris-buffered saline (TBS) and 5% milk for at least 30 min. Primary antibodies are diluted to appropriate concentration in TBS with 0.5% Tween-20 (TBST) with 5% milk and incubated overnight at 4 °C. Membranes are washed 3X in TBST and then incubated with appropriate HRP-conjugated secondary antibody (Life Technologies) at 1:10 000 dilution in TBST/milk for 1 h at room temperature. Membranes are washed 3× with TBST, then developed using Amersham ECL Prime (GE Life Sciences). Blots are imaged using the BioRad Versadoc imager and analyzed using Image Lab software. Antibodies: GAPDH (AB2302, Millipore); H3K27me3 (07−449, Millipore); H3K27ac (39125, Active Motif); total H3 (ab1791, Abcam).

MNase Chromatin Immunoprecipitation (ChIP). MNase ChIP was performed as described previously (Skene and Henikoff, 2015).[51] Briefly, 5×10^6 cells (2D10, JLat6.3 and JLatA2) were treated with 10 μM EED inhibitor for 72 h in combination with SAHA for the last 24 h. Cells were fixed with 1% formaldehyde for 10 min and quenched with 125 mM glycine for 15 min. Cell pellets were washed with ice cold PBS three times and frozen at −80 °C. Cells were resuspended in 150 μL ice cold lysis buffer [1% SDS, 10 mM EDTA and 50 mM Tris-HCl (pH 8.1)] containing protease inhibitors and lysed on ice for 15 min. To each tube, 1350 μL of ice cold ChIP dilution buffer [1% Triton X100, 2 mM EDTA, 150 mM NaCl and 20 mM Tris-HCl (pH 8.1)] containing 3 mM $CaCl_2$ was added. Tubes were place at 37 °C for 5 min prior to addition of 2.5 μL of MNase (10 U/μL) for 10 min and the reactions were stopped by adding 30 μL EDTA and 60 μL EGTA. The tubes were spun at 16 000 rpm at 4 °C and the soluble extract was collected. 200 μL of the soluble supernatant was incubated with 2 μL of H3, 5 μL of H3K27me3 and 2 μL of H3K27Ac antibodies overnight at 4 °C. The next day, Protein G Dynabeads (Invitrogen) were added to the supernatants for 2 h. The antigen−antibody complexes were washed successively once (1×) with TSE1 buffer [0.1% SDS, 1% Triton X100, 2 mM EDTA, 20 mM Tris-HCl (pH 8.1) and 150 mM NaCl], four times (4×) with TSE2 [0.1% SDS, 1%

https://dx.doi.org/10.1021/acsinfecdis.9b00514
ACS Infect. Dis. 2020, 6, 1719−1733

Triton X100, 2 mM EDTA, 20 mM Tris-HCl (pH 8.1) and 500 mM NaCl], once (1×) with Buffer III [0.25 M LiCl, 1% NP40, 1% Sodium Deoxycholate, 1 mM EDTA, 10 mM Tris-HCl (pH 8.1)] followed by three washes with TE buffer. DNA−protein complexes were eluted from the beads using elution buffer (0.1 M $NaHCO_3$ and 1% SDS) and de-cross-linked overnight at 65 °C. DNA was extracted using ChIP Clean and Concentrator Kits (Zymo Research). qPCR was performed as described previously using SYBR green (Biorad) and the signal obtained was normalized to the input and then to total H3 signal. Primers sets for Nuc0[10] (F-5′ ACACA-CAAGGCTACTTCCCTG, R-5′ TCTACCTTATCTGGC-TCAACTGGT), Nuc1[47] (F-5′ TCTCTGGCTAACTAG-GGAACC, R-5′ AAAGGGTCTGAGGGATCTCTAG), and Nuc2[47] (F-5′ AGAGATGGGTGCGAGAGC, R-5′ ATTAA-CTGCGAATCGTTCTAGC) are previously published. Two independent ChIP experiments were performed, each with three biological replicates, and the data are represented as the mean ± standard error of the mean.

Primary Cell Assays. Total CD4+ cells were obtained using the EasySep Human CD4+ T Cell Isolation Kit (Stemcell Technologies) per the manufacturer's protocol after standard isolation of peripheral blood mononuclear cells via Ficoll-Paque (GE Lifesciences) from anonymous, healthy blood donors (New York Blood Center). Seven million total CD4+ cells were treated with EEDi (A-395 or EED226) or EZH2i (UNC1999 or GSK343) at indicated concentrations for each time point assayed. Lymphocytes were obtained from aviremic HIV+ individuals on stable antiretroviral therapy by continuous-flow leukapheresis and resting CD4+ T cells isolated as previously described.[48] Written consent was obtained from all participants and protocols used to obtain leukapheresis was approved by the University of North Carolina Biomedical Institutional Review Board. Resting and total CD4+ T cells were treated for 96 h with EED226 and A-395 in IMDM/10%FBS/Pen/Strep with 10 U/mL IL-2 with the addition of SAHA and PMA/Ionomycin or 3 μg/mL PHA for the final 24 h. RNA was isolated from 8 to 12 replicates of 1 million resting cells (Donors 1 and 2) or 1 million total CD4+ cells (Donor 4) using the MagMax-96 Total RNA Isolation Kit (Life Technologies) following the manufacturer's protocol. Three replicates of 4 million total CD4+ cells from Donor 3 were isolated using the RNeasy Mini RNA Isolation Kit (Qiagen) per manufacturer's protocol. cDNA was synthesized in duplicate from DNase-treated, isolated RNA using the SuperScript III First-Strand Synthesis SuperMix kit (Life Technologies) according to the manufacturer's procedures. PCR amplification of pooled cDNA was performed in technical triplicates using the Biorad FX96 Real-Time PCR machine and previously published primers and probe.[49] A standard curve was generated for each PCR reaction as described previously.[50]

Activation Markers. Total CD4+ cells were obtained using the EasySep Human CD4+ T Cell Isolation Kit (Stemcell Technologies) per manufacturers protocol after standard isolation of peripheral blood mononuclear cells via Ficoll-Paque (GE Lifesciences) from anonymous, healthy blood donors (New York Blood Center). Cells were treated with EED or EZH2 inhibitors at indicated dosages and time points at a concentration of 3E6/mL. 90uL of cells were subject to alamarBlue assay (Life Technologies) per the manufacturer's instructions. Samples incubated for 2 h at 37 °C, followed by fluorescence detection at $560_{EX}/590_{EM}$ using a SpectraMax M3 (Molecular Devices). The remaining cells were stained with Live/Dead NIR (Life Technologies), CD4-PE (Clone RPA-T4, BD Biosciences), CD3-PerCP-Cy5.5 (Clone UCHT1, Biolegend), CD25-FITC (Clone BC96, Biolegend), and CD69-APC (Clone FN50, Biolegend). Unstained and FMO controls were generated using PHA stimulated cells for each experiment and all flow was run on an Attune NXT with data analysis performed using FlowJo.

Statistical Analysis. All analysis was performed using Graphpad Prism. *p*-values were determined using the non-parametric Mann−Whitney U Test for samples with an $n \geq 5$.

■ ASSOCIATED CONTENT

Supporting Information

The Supporting Information is available free of charge at https://pubs.acs.org/doi/10.1021/acsinfecdis.9b00514.

Supplementary Figures S1−S6 and chemistry experimental section including LCMS and NMR spectra (PDF)

■ AUTHOR INFORMATION

Corresponding Authors

David M. Margolis − *UNC HIV Cure Center, Department of Medicine, and Department of Microbiology and Immunology, University of North Carolina at Chapel Hill School of Medicine, Chapel Hill, North Carolina 27599, United States; Department of Epidemiology, University of North Carolina at Chapel Hill School of Public Health, Chapel Hill, North Carolina 27599, United States*; Phone: (919) 966-6388; Email: dmargo@med.unc.edu

Lindsey I. James − *UNC HIV Cure Center, University of North Carolina at Chapel Hill School of Medicine, Chapel Hill, North Carolina 27599, United States; Center for Integrative Chemical Biology and Drug Discovery, Division of Chemical Biology and Medicinal Chemistry, Eshelman School of Pharmacy, University of North Carolina at Chapel Hill, Chapel Hill, North Carolina 27599, United States*; orcid.org/0000-0002-6034-7116; Phone: (919) 962-4870; Email: ingerman@email.unc.edu

Authors

Anne-Marie W. Turner − *UNC HIV Cure Center and Department of Medicine, University of North Carolina at Chapel Hill School of Medicine, Chapel Hill, North Carolina 27599, United States*

Raghuvar Dronamraju − *Department of Biochemistry & Biophysics, University of North Carolina at Chapel Hill School of Medicine, Chapel Hill, North Carolina 27599, United States*

Frances Potjewyd − *Center for Integrative Chemical Biology and Drug Discovery, Division of Chemical Biology and Medicinal Chemistry, Eshelman School of Pharmacy, University of North Carolina at Chapel Hill, Chapel Hill, North Carolina 27599, United States*

Katherine S. James − *UNC HIV Cure Center, University of North Carolina at Chapel Hill School of Medicine, Chapel Hill, North Carolina 27599, United States*

Daniel K. Winecoff − *UNC HIV Cure Center, University of North Carolina at Chapel Hill School of Medicine, Chapel Hill, North Carolina 27599, United States*

Jennifer L. Kirchherr − *UNC HIV Cure Center, University of North Carolina at Chapel Hill School of Medicine, Chapel Hill, North Carolina 27599, United States*

https://dx.doi.org/10.1021/acsinfecdis.9b00514
ACS Infect. Dis. 2020, 6, 1719−1733

Nancie M. Archin − *UNC HIV Cure Center and Department of Medicine, University of North Carolina at Chapel Hill School of Medicine, Chapel Hill, North Carolina 27599, United States*
Edward P. Browne − *UNC HIV Cure Center and Department of Medicine, University of North Carolina at Chapel Hill School of Medicine, Chapel Hill, North Carolina 27599, United States*
Brian D. Strahl − *Department of Biochemistry & Biophysics, University of North Carolina at Chapel Hill School of Medicine, Chapel Hill, North Carolina 27599, United States;* orcid.org/0000-0002-4947-6259

Complete contact information is available at: https://pubs.acs.org/10.1021/acsinfecdis.9b00514

Notes

The authors declare no competing financial interest.

■ ACKNOWLEDGMENTS

The authors thank members of the James, Strahl, and Margolis laboratories for technical assistance. The authors are also grateful for assistance by the UNC Center for AIDS Research Biostatistics Core, specifically K. Mollan and A.K. Weideman, supported by award number P30 AI050410. The authors thank the Structural Genomics Consortium for sharing A-395 for some of these studies. This work was supported by CARE, a Martin Delaney Collaboratory of the National Institute of Allergy and Infectious Diseases (NIAID), the National Institute of Neurological Disorders and Stroke (NINDS), the National Institute on Drug Abuse (NIDA), and the National Institute of Mental Health (NIMH) of the National Institutes of Health, grant number 1UM1AI126619-01 to D.M.M. This work was also supported by the National Institute on Drug Abuse (NIDA) of the National Institutes of Health under award number 1R61DA047023-01 to L.I.J. A.W.T. was supported by the National Institute of Allergy and Infectious Diseases (NIAID) of the National Institutes of Health under award number T32AI007001. Work in the UNC Flow Cytometry Core Facility is supported in part by the Center for AIDS Research award number P30-AI050410 and the North Carolina Biotech Center Institutional Support Grant 2015-IDG-1001.

■ REFERENCES

(1) Margolis, D. M., Garcia, J. V., Hazuda, D. J., and Haynes, B. F. (2016) Latency reversal and viral clearance to cure HIV-1. *Science 353*, aaf6517.
(2) Muller, J., and Verrijzer, P. (2009) Biochemical mechanisms of gene regulation by polycomb group protein complexes. *Curr. Opin. Genet. Dev. 19*, 150−158.
(3) Sparmann, A., and van Lohuizen, M. (2006) Polycomb silencers control cell fate, development and cancer. *Nat. Rev. Cancer 6*, 846−856.
(4) Cao, R., and Zhang, Y. (2004) SUZ12 Is Required for Both the Histone Methyltransferase Activity and the Silencing Function of the EED-EZH2 Complex. *Mol. Cell 15*, 57−67.
(5) Margueron, R., Justin, N., Ohno, K., Sharpe, M. L., Son, J., Drury, W. J., 3rd, Voigt, P., Martin, S. R., Taylor, W. R., De Marco, V., Pirrotta, V., Reinberg, D., and Gamblin, S. J. (2009) Role of the polycomb protein EED in the propagation of repressive histone marks. *Nature 461*, 762−767.
(6) Moritz, L. E., and Trievel, R. C. (2018) Structure, mechanism, and regulation of polycomb-repressive complex 2. *J. Biol. Chem. 293*, 13805−13814.
(7) Blackledge, N. P., Rose, N. R., and Klose, R. J. (2015) Targeting Polycomb systems to regulate gene expression: modifications to a complex story. *Nat. Rev. Mol. Cell Biol. 16*, 643−649.
(8) Tavares, L., Dimitrova, E., Oxley, D., Webster, J., Poot, R., Demmers, J., Bezstarosti, K., Taylor, S., Ura, H., Koide, H., Wutz, A., Vidal, M., Elderkin, S., and Brockdorff, N. (2012) RYBP-PRC1 Complexes Mediate H2A Ubiquitylation at Polycomb Target Sites Independently of PRC2 and H3K27me3. *Cell 148*, 664−678.
(9) Cooper, S., Grijzenhout, A., Underwood, E., Ancelin, K., Zhang, T., Nesterova, T. B., Anil-Kirmizitas, B., Bassett, A., Kooistra, S. M., Agger, K., Helin, K., Heard, E., and Brockdorff, N. (2016) Jarid2 binds mono-ubiquitylated H2A lysine 119 to mediate crosstalk between Polycomb complexes PRC1 and PRC2. *Nat. Commun. 7*, 13661.
(10) Friedman, J., Cho, W.-K., Chu, C. K., Keedy, K. S., Archin, N. M., Margolis, D. M., and Karn, J. (2011) Epigenetic Silencing of HIV-1 by the Histone H3 Lysine 27 Methyltransferase Enhancer of Zeste 2. *J. Virol. 85*, 9078−9089.
(11) Pearson, R., Kim, Y. K., Hokello, J., Lassen, K., Friedman, J., Tyagi, M., and Karn, J. (2008) Epigenetic Silencing of Human Immunodeficiency Virus (HIV) Transcription by Formation of Restrictive Chromatin Structures at the Viral Long Terminal Repeat Drives the Progressive Entry of HIV into Latency. *J. Virol. 82*, 12291−12303.
(12) Tripathy, M. K., McManamy, M. E. M., Burch, B. D., Archin, N. M., and Margolis, D. M. (2015) H3K27 Demethylation at the Proviral Promoter Sensitizes Latent HIV to the Effects of Vorinostat in Ex Vivo Cultures of Resting CD4+ T Cells. *J. Virol. 89*, 8392−8405.
(13) Matsuda, Y., Kobayashi-Ishihara, M., Fujikawa, D., Ishida, T., Watanabe, T., and Yamagishi, M. (2015) Epigenetic Heterogeneity in HIV-1 Latency Establishment. *Sci. Rep. 5*, 7701.
(14) Nguyen, K., Das, B., Dobrowolski, C., and Karn, J. (2017) Multiple Histone Lysine Methyltransferases Are Required for the Establishment and Maintenance of HIV-1 Latency. *mBio 8*, e00133−00117.
(15) He, Y., Selvaraju, S., Curtin, M. L., Jakob, C. G., Zhu, H., Comess, K. M., Shaw, B., The, J., Lima-Fernandes, E., Szewczyk, M. M., Cheng, D., Klinge, K. L., Li, H.-Q., Pliushchev, M., Algire, M. A., Maag, D., Guo, J., Dietrich, J., Panchal, S. C., Petros, A. M., Sweis, R. F., Torrent, M., Bigelow, L. J., Senisterra, G., Li, F., Kennedy, S., Wu, Q., Osterling, D. J., Lindley, D. J., Gao, W., Galasinski, S., Barsyte-Lovejoy, D., Vedadi, M., Buchanan, F. G., Arrowsmith, C. H., Chiang, G. G., Sun, C., and Pappano, W. N. (2017) The EED protein-protein interaction inhibitor A-395 inactivates the PRC2 complex. *Nat. Chem. Biol. 13*, 389−395.
(16) Qi, W., Zhao, K., Gu, J., Huang, Y., Wang, Y., Zhang, H., Zhang, M., Zhang, J., Yu, Z., Li, L., Teng, L., Chuai, S., Zhang, C., Zhao, M., Chan, H., Chen, Z., Fang, D., Fei, Q., Feng, L., Feng, L., Gao, Y., Ge, H., Ge, X., Li, G., Lingel, A., Lin, Y., Liu, Y., Luo, F., Shi, M., Wang, L., Wang, Z., Yu, Y., Zeng, J., Zeng, C., Zhang, L., Zhang, Q., Zhou, S., Oyang, C., Atadja, P., and Li, E. (2017) An allosteric PRC2 inhibitor targeting the H3K27me3 binding pocket of EED. *Nat. Chem. Biol. 13*, 381−388.
(17) Huang, Y., Zhang, J., Yu, Z., Zhang, H., Wang, Y., Lingel, A., Qi, W., Gu, J., Zhao, K., Shultz, M. D., Wang, L., Fu, X., Sun, Y., Zhang, Q., Jiang, X., Zhang, J., Zhang, C., Li, L., Zeng, J., Feng, L., Zhang, C., Liu, Y., Zhang, M., Zhang, L., Zhao, M., Gao, Z., Liu, X., Fang, D., Guo, H., Mi, Y., Gabriel, T., Dillon, M. P., Atadja, P., and Oyang, C. (2017) Discovery of First-in-Class, Potent, and Orally Bioavailable Embryonic Ectoderm Development (EED) Inhibitor with Robust Anticancer Efficacy. *J. Med. Chem. 60*, 2215−2226.
(18) Laird, G. M., Bullen, C. K., Rosenbloom, D. I., Martin, A. R., Hill, A. L., Durand, C. M., Siliciano, J. D., and Siliciano, R. F. (2015) Ex vivo analysis identifies effective HIV-1 latency-reversing drug combinations. *J. Clin. Invest. 125*, 1901−1912.
(19) Archin, N. M., Cheema, M., Parker, D., Wiegand, A., Bosch, R. J., Coffin, J. M., Eron, J., Cohen, M., and Margolis, D. M. (2010) Antiretroviral intensification and valproic acid lack sustained effect on

residual HIV-1 viremia or resting CD4+ cell infection. *PLoS One 5*, e9390.
(20) Archin, N. M., Espeseth, A., Parker, D., Cheema, M., Hazuda, D., and Margolis, D. M. (2009) Expression of latent HIV induced by the potent HDAC inhibitor suberoylanilide hydroxamic acid. *AIDS Res. Hum. Retroviruses 25*, 207−212.
(21) Archin, N. M., Kirchherr, J. L., Sung, J. A. M., Clutton, G., Sholtis, K., Xu, Y., Allard, B., Stuelke, E., Kashuba, A. D., Kuruc, J. D., Eron, J., Gay, C. L., Goonetilleke, N., and Margolis, D. M. (2017) Interval dosing with the HDAC inhibitor vorinostat effectively reverses HIV latency. *J. Clin. Invest. 127*, 3126−3135.
(22) Jordan, A., Bisgrove, D., and Verdin, E. (2003) HIV reproducibly establishes a latent infection after acute infection of T cells in vitro. *EMBO J. 22*, 1868−1877.
(23) Jordan, A., Defechereux, P., and Verdin, E. (2001) The site of HIV-1 integration in the human genome determines basal transcriptional activity and response to Tat transactivation. *EMBO J. 20*, 1726−1738.
(24) Spina, C. A., Anderson, J., Archin, N. M., Bosque, A., Chan, J., Famiglietti, M., Greene, W. C., Kashuba, A., Lewin, S. R., Margolis, D. M., Mau, M., Ruelas, D., Saleh, S., Shirakawa, K., Siliciano, R. F., Singhania, A., Soto, P. C., Terry, V. H., Verdin, E., Woelk, C., Wooden, S., Xing, S., and Planelles, V. (2013) An In-Depth Comparison of Latent HIV-1 Reactivation in Multiple Cell Model Systems and Resting CD4+ T Cells from Aviremic Patients. *PLoS Pathog. 9*, e1003834.
(25) Verma, S. K., Tian, X., LaFrance, L. V., Duquenne, C., Suarez, D. P., Newlander, K. A., Romeril, S. P., Burgess, J. L., Grant, S. W., Brackley, J. A., Graves, A. P., Scherzer, D. A., Shu, A., Thompson, C., Ott, H. M., Aller, G. S. V., Machutta, C. A., Diaz, E., Jiang, Y., Johnson, N. W., Knight, S. D., Kruger, R. G., McCabe, M. T., Dhanak, D., Tummino, P. J., Creasy, C. L., and Miller, W. H. (2012) Identification of Potent, Selective, Cell-Active Inhibitors of the Histone Lysine Methyltransferase EZH2. *ACS Med. Chem. Lett. 3*, 1091−1096.
(26) Konze, K. D., Ma, A., Li, F., Barsyte-Lovejoy, D., Parton, T., MacNevin, C. J., Liu, F., Gao, C., Huang, X.-P., Kuznetsova, E., Rougie, M., Jiang, A., Pattenden, S. G., Norris, J. L., James, L. I., Roth, B. L., Brown, P. J., Frye, S. V., Arrowsmith, C. H., Hahn, K. M., Wang, G. G., Vedadi, M., and Jin, J. (2013) An Orally Bioavailable Chemical Probe of the Lysine Methyltransferases EZH2 and EZH1. *ACS Chem. Biol. 8*, 1324−1334.
(27) Mbonye, U., and Karn, J. (2011) Control of HIV latency by epigenetic and non-epigenetic mechanisms. *Curr. HIV Res. 9*, 554−567.
(28) Turner, A.-M. W., and Margolis, D. M. (2017) Chromatin Regulation and the Histone Code in HIV Latency. *Yale J. Biol. Med. 90*, 229−243.
(29) Pasini, D., Malatesta, M., Jung, H. R., Walfridsson, J., Willer, A., Olsson, L., Skotte, J., Wutz, A., Porse, B., Jensen, O. N., and Helin, K. (2010) Characterization of an antagonistic switch between histone H3 lysine 27 methylation and acetylation in the transcriptional regulation of Polycomb group target genes. *Nucleic Acids Res. 38*, 4958−4969.
(30) Huang, X., Yan, J., Zhang, M., Wang, Y., Chen, Y., Fu, X., Wei, R., Zheng, X.-l., Liu, Z., Zhang, X., Yang, H., Hao, B., Shen, Y.-y., Su, Y., Cong, X., Huang, M., Tan, M., Ding, J., and Geng, M. (2018) Targeting Epigenetic Crosstalk as a Therapeutic Strategy for EZH2-Aberrant Solid Tumors. *Cell 175*, 186−199.
(31) Hottiger, M. O., and Nabel, G. J. (1998) Interaction of human immunodeficiency virus type 1 Tat with the transcriptional coactivators p300 and CREB binding protein. *J. Virol. 72*, 8252−8256.
(32) Lusic, M., Marcello, A., Cereseto, A., and Giacca, M. (2003) Regulation of HIV-1 gene expression by histone acetylation and factor recruitment at the LTR promoter. *EMBO J. 22*, 6550−6561.
(33) Marzio, G., Tyagi, M., Gutierrez, M. I., and Giacca, M. (1998) HIV-1 tat transactivator recruits p300 and CREB-binding protein histone acetyltransferases to the viral promoter. *Proc. Natl. Acad. Sci. U. S. A. 95*, 13519−13524.
(34) Cillo, A. R., Sobolewski, M. D., Bosch, R. J., Fyne, E., Piatak, M., Coffin, J. M., and Mellors, J. W. (2014) Quantification of HIV-1 latency reversal in resting CD4+ T cells from patients on suppressive antiretroviral therapy. *Proc. Natl. Acad. Sci. U. S. A. 111*, 7078−7083.
(35) Kauder, S. E., Bosque, A., Lindqvist, A., Planelles, V., and Verdin, E. (2009) Epigenetic Regulation of HIV-1 Latency by Cytosine Methylation. *PLoS Pathog. 5*, e1000495.
(36) Bednarik, D. P., Cook, J. A., and Pitha, P. M. (1990) Inactivation of the HIV LTR by DNA CpG methylation: evidence for a role in latency. *EMBO J. 9*, 1157−1164.
(37) Bednarik, D. P., Mosca, J. D., and Raj, N. B. (1987) Methylation as a modulator of expression of human immunodeficiency virus. *J. Virol. 61*, 1253−1257.
(38) Clutton, G., Xu, Y., Baldoni, P. L., Mollan, K. R., Kirchherr, J., Newhard, W., Cox, K., Kuruc, J. D., Kashuba, A., Barnard, R., Archin, N., Gay, C. L., Hudgens, M. G., Margolis, D. M., and Goonetilleke, N. (2016) The differential short- and long-term effects of HIV-1 latency-reversing agents on T cell function. *Sci. Rep. 6*, 30749.
(39) Jadhav, U., Manieri, E., Nalapareddy, K., Madha, S., Chakrabarti, S., Wucherpfennig, K., Barefoot, M., and Shivdasani, R. A. (2020) Replicational Dilution of H3K27me3 in Mammalian Cells and the Role of Poised Promoters. *Mol. Cell 78*, 141.
(40) Kim, J., Lee, Y., Lu, X., Song, B., Fong, K.-W., Cao, Q., Licht, J. D., Zhao, J. C., and Yu, J. (2018) Polycomb- and Methylation-Independent Roles of EZH2 as a Transcription Activator. *Cell Rep. 25*, 2808−2820.
(41) Kim, K. H., Kim, W., Howard, T. P., Vazquez, F., Tsherniak, A., Wu, J. N., Wang, W., Haswell, J. R., Walensky, L. D., Hahn, W. C., Orkin, S. H., and Roberts, C. W. M. (2015) SWI/SNF-mutant cancers depend on catalytic and non-catalytic activity of EZH2. *Nat. Med. 21*, 1491−1497.
(42) Xu, K., Wu, Z. J., Groner, A. C., He, H. H., Cai, C., Lis, R. T., Wu, X., Stack, E. C., Loda, M., Liu, T., Xu, H., Cato, L., Thornton, J. E., Gregory, R. I., Morrissey, C., Vessella, R. L., Montironi, R., Magi-Galluzzi, C., Kantoff, P. W., Balk, S. P., Liu, X. S., and Brown, M. (2012) EZH2 Oncogenic Activity in Castration-Resistant Prostate Cancer Cells Is Polycomb-Independent. *Science 338*, 1465−1469.
(43) Baker, T., Nerle, S., Pritchard, J., Zhao, B., Rivera, V. M., Garner, A., and Gonzalvez, F. (2015) Acquisition of a single EZH2 D1 domain mutation confers acquired resistance to EZH2-targeted inhibitors. *Oncotarget 6*, 32646−32655.
(44) Gibaja, V., Shen, F., Harari, J., Korn, J., Ruddy, D., Saenz-Vash, V., Zhai, H., Rejtar, T., Paris, C. G., Yu, Z., Lira, M., King, D., Qi, W., Keen, N., Hassan, A. Q., and Chan, H. M. (2016) Development of secondary mutations in wild-type and mutant EZH2 alleles cooperates to confer resistance to EZH2 inhibitors. *Oncogene 35*, 558−566.
(45) BLISS, C. I. (1939) THE TOXICITY OF POISONS APPLIED JOINTLY1. *Ann. Appl. Biol. 26*, 585−615.
(46) Jiang, G., Mendes, E. A., Kaiser, P., Wong, D. P., Tang, Y., Cai, I., Fenton, A., Melcher, G. P., Hildreth, J. E. K., Thompson, G. R., Wong, J. K., and Dandekar, S. (2015) Synergistic Reactivation of Latent HIV Expression by Ingenol-3-Angelate, PEP005, Targeted NF-kB Signaling in Combination with JQ1 Induced p-TEFb Activation. *PLoS Pathog. 11*, e1005066.
(47) Rafati, H., Parra, M., Hakre, S., Moshkin, Y., Verdin, E., and Mahmoudi, T. (2011) Repressive LTR nucleosome positioning by the BAF complex is required for HIV latency. *PLoS Biol. 9*, e1001206.
(48) Keedy, K. S., Archin, N. M., Gates, A. T., Espeseth, A., Hazuda, D. J., and Margolis, D. M. (2009) A Limited Group of Class I Histone Deacetylases Acts To Repress Human Immunodeficiency Virus Type 1 Expression. *J. Virol. 83*, 4749−4756.
(49) Israel-Ballard, K., Ziermann, R., Leutenegger, C., Di Canzio, J., Leung, K., Strom, L., Abrams, B., and Chantry, C. (2005) TaqMan RT-PCR and VERSANT® HIV-1 RNA 3.0 (bDNA) assay: Quantification of HIV-1 RNA viral load in breast milk. *J. Clin. Virol. 34*, 253−256.
(50) Archin, N. M., Liberty, A. L., Kashuba, A. D., Choudhary, S. K., Kuruc, J. D., Crooks, A. M., Parker, D. C., Anderson, E. M., Kearney, M. F., Strain, M. C., Richman, D. D., Hudgens, M. G., Bosch, R. J.,

https://dx.doi.org/10.1021/acsinfecdis.9b00514
ACS Infect. Dis. 2020, 6, 1719−1733

Coffin, J. M., Eron, J. J., Hazuda, D. J., and Margolis, D. M. (2012) Administration of vorinostat disrupts HIV-1 latency in patients on antiretroviral therapy. *Nature 487*, 482−485.
(51) Skene, P. J., and Henikoff, S. (2015) A simple method for generating high-resolution maps of genome-wide protein binding. *eLife*, DOI: 10.7554/eLife.09225.

https://dx.doi.org/10.1021/acsinfecdis.9b00514
ACS Infect. Dis. 2020, 6, 1719−1733